International Journal of Computational and Experimental Science and ENgineering (IJCESEN)

Vol. 11-No.2 (2025) pp. 3486-3493

http://www.ijcesen.com

ISSN: 2149-9144

Research Article

Numerical investigation of perforated aluminium tubes with different types of geometrical discontinuities under bending

Çetin Karakaya[1], Seçil Ekşi[2]*

[1] Independent Researcher, Hastings, United Kingdom
Email: cetkarakaya@gmail.com **- ORCID:**0000-0002-9227-9170

[2]Mechanical Engineering Department, Sakarya University, Sakarya, 54050, Turkey
* **Corresponding Author Email:** eksi@sakarya.edu.tr - **ORCID**: 0000-0002-1404-718X

Article Info:

DOI: 10.22399/ijcesen.2237
Received : 21 March 2025
Accepted : 05 May 2025

Keywords :

Aluminum, Bending
Perforated tube
Hole shape
Finite element analysis

Abstract:

In this study, the effect of hole shape on the bending behavior of aluminum 6063-T5 tubes was investigated numerically. The effects of hole geometries in the form of circles, triangles, squares, hexagons, ellipses, and diamonds on the bending behavior of the tube structure were investigated by finite element analysis. As a result of the analysis, the tube structure with the highest load-carrying and energy-absorption capacity is the ellipse perforated tube. In terms of specific load carrying and specific energy absorption capacity, the ellipse perforated tube structure is again in first place. Compared to the non-perforated tube, the load carrying capacity has decreased by 13.6%, and the energy absorption capacity has decreased by 11%. The triangular perforated structure comes in second place. The square perforated tube is in last place.

1. Introduction

Lightweight, energy-efficient structural components are increasingly essential in transportation, aerospace, and defense industries, where weight reduction must be balanced with structural integrity and crashworthiness. Thin-walled aluminum tubes, owing to their excellent strength-to-weight ratio, corrosion resistance, and formability, have been extensively studied for applications in energy absorption systems, crash boxes, and structural frames [1–3]. While the mechanical behavior of such tubes under axial compression is well-documented [4–6], the response under bending, especially in the presence of perforations, remains a relatively underexplored field.

Bending loads are prevalent in real-world applications, such as side impacts in automotive collisions or bending architectural support elements. Under such loading, thin-walled tubes exhibit complex deformation mechanisms, including ovalization, local buckling, and plastic hinge formation [7–9]. These failure modes are susceptible to the geometry, material properties, and loading conditions [10–12]. Perforations, introduced either for functional purposes (e.g., ventilation, wiring) or as a design strategy for controlled collapse, further complicate this response by altering stiffness, stress distribution, and buckling patterns [13–15].

The integration of holes in tube structures has been studied with growing interest, particularly in axial and lateral crushing. Alavi Nia and Hoseini [16] systematically analyzed the collapse of cylindrical tubes with different hole patterns, demonstrating how perforation can trigger desired collapse mechanisms, enhancing energy absorption. Similarly, Kim et al. [17] and Hwang et al. [18] examined the crashworthiness of perforated tubes and reported that hole geometry, spacing, and distribution directly influence deformation behavior and load-bearing capacity. Nevertheless, most of these studies focused on axial compression or quasi-static crushing; few addressed bending, where hole placement can shift plastic hinge locations or cause premature buckling [19–21].

Several researchers have explored foam-filled, multi-cell, and triggered geometries to enhance energy dissipation [22–24]. However, perforated tubes offer a passive and potentially lighter-weight alternative, with design tunability via hole size, shape, and layout. Li et al. [25] and Zarei and Kröger [26] highlighted the importance of geometry tailoring for enhancing structural performance. More recently, Boria et al. [27] and Fang et al. [28] extended this concept using non-circular and irregular perforation shapes, showing promising results under axial and combined loadings. However, the effect of different hole types under bending, especially using robust numerical models, remains under-investigated.

Accurate modeling of perforated tubes under bending requires advanced numerical techniques, particularly Finite Element Method (FEM) simulations capable of capturing localized effects like stress concentrations, buckling initiation, and plastic hinge evolution [29–31]. FEM allows parametric studies that are often infeasible experimentally. Zhao and Elnashai [32] and Langseth et al. [33] demonstrated the reliability of numerical models in predicting post-buckling behavior of complex structures. Nonetheless, mesh refinement near holes, proper failure criteria, and material calibration are critical for meaningful predictions [34–36].

Recent studies also highlight the impact of strain rate effects, boundary conditions, and initial imperfections on bending behavior [37–39]. Yet, the combined effect of these parameters with varying hole types — such as circular, square, elliptical, or hexagonal holes — is still an open question. The absence of systematic numerical investigations into these parameters under bending motivates the current study.

This study aims to systematically investigate the bending behavior of perforated aluminum tubes with varying hole shapes. The research employs finite element simulations to evaluate how perforation shapes influence bending strength, bending stiffness, load carrying capacity, and energy absorption capacity. Through this comprehensive approach, the work contributes to optimizing perforated tube designs for lightweight and crashworthy applications in transportation and structural engineering applications.

2. Validation Study

The tube used in the validation study in experiments is Al 6063-T5. The outer diameter is 31 mm, the wall thickness is 1 mm, and the length of the cylindrical aluminum tube is 270 mm, respectively. The material used for the tube is Al 6063-T5 with the following properties: mass density ρ = 2.7 g × cm-3, Young's modulus E = 69 GPa, yield strength σ_Y = 187 MPa, ultimate stress σ_U = 247 MPa, Poisson's ratio ν = 0.33. A tensile test for the aluminum tube was carried out using specimens prepared according to the ASTM E8 standard. A video extensometer was used in tension test programs. Three-point bending tests were carried out on a 10 kN bending test machine to determine the bending behavior of tubes. The diameter of the punch and supports was set to be 30 mm, which was suitable for the tube diameter. The span of the two supports was 217 mm. The loading rate was kept constant at 0.5 mm × s-1.

The finite element model is generated and analyzed using ANSYS. In this model, the The full model was generated without using symmetry assumptions, which resulted in 10371 3-D 20-node solid elements (Solid186) and 63005 nodes for the tubular beam, supports, and the loading punch. Since the problem involves large deformation, the nonlinear geometry is also turned on during the analysis. The coefficient of friction between the contacting surfaces is taken as σ = 0.2. Figure 2 represents load-displacement curves from the experiment and finite element simulations. The load magnitudes between the experiment and simulation differ by ~1.5 %. From the above comparison, it is clear that the finite element model and simulation methodology used are valid, and therefore, the method and similar models can be used to study the behavior of other similar systems for different material properties. Figure 1 shows the experimental setup used for the three-point bending test and the finite element analysis model.

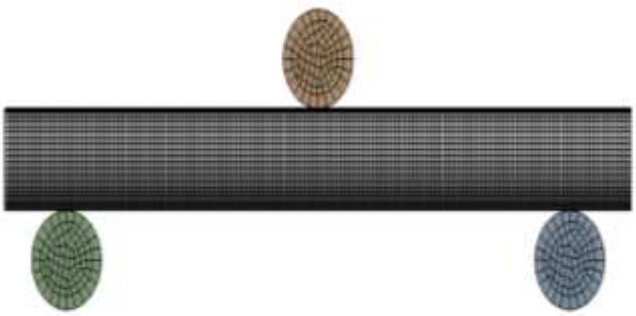

Figure 1. *a) Experimental set-up for three-point bending validation test, b) Finite element analysis model*

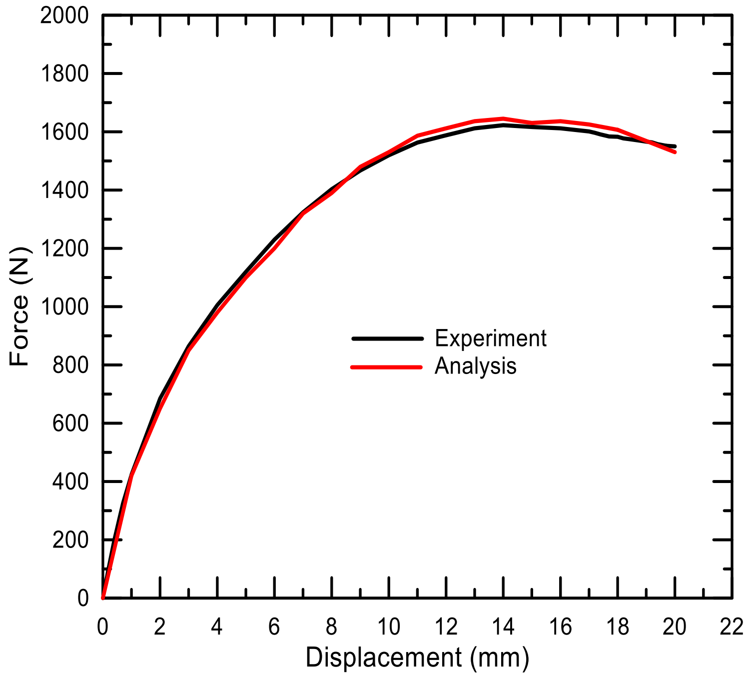

Figure 2. *Force-displacement curves from the experiment and finite element simulation*

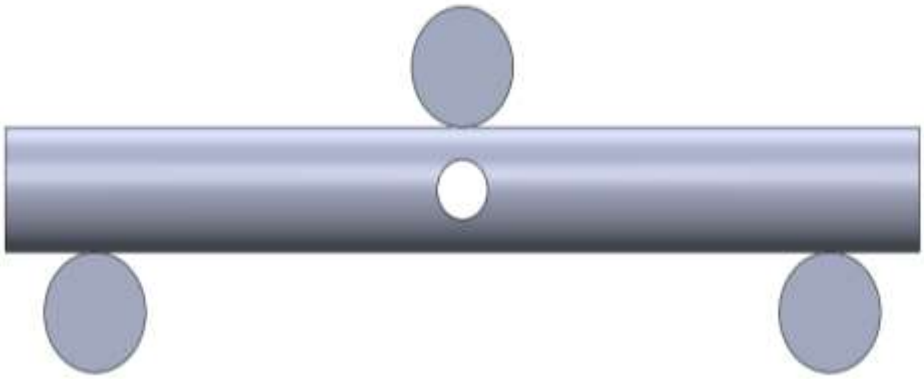

Figure 3. *Finite element analysis models of perforated tubes*

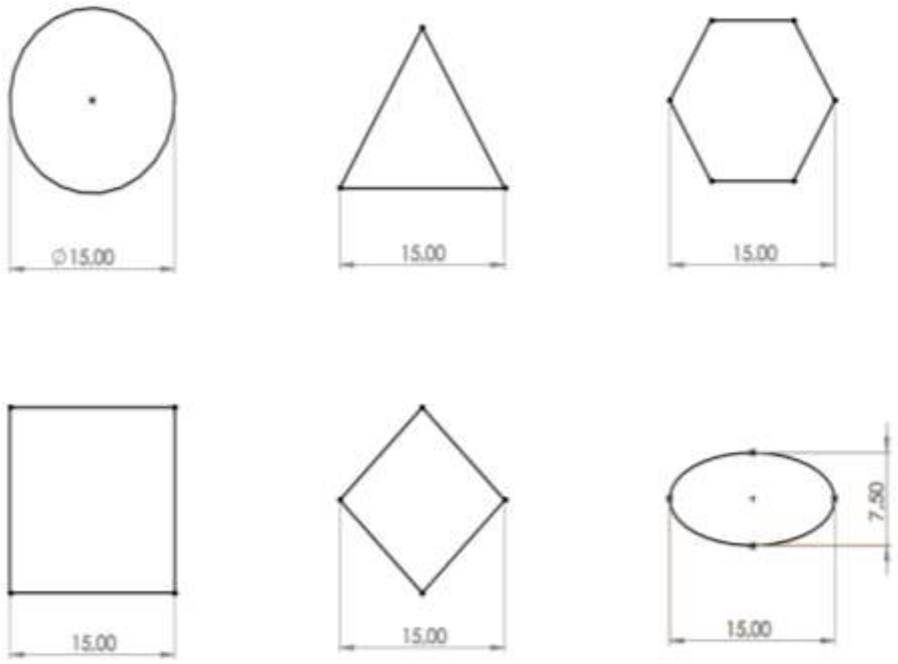

Figure 4. *Hole shapes for a perforated tube*

3. Numerical Study

Material properties and the dimensions of the tube structure used in finite element analyses are the same as the tube used in the validation study. The outer diameter is 31 mm, the wall thickness is 1 mm, and the length of the cylindrical aluminum tube is 270 mm, respectively. The span of the two supports was 217 mm. The diameter of the punch and supports was 30 mm.
The finite element models are generated and analyzed using ANSYS. The finite element analysis model of the perforated tubes with circular hole shape is shown in Figure 3. Hole shapes for perforated tubes are given in Figure 4.
To investigate the performance of tube structures under three-point bending, four parameters - load carrying capacity (LC), specific load carrying capacity (SLC), energy absorption (EA), and specific energy absorption (SEA) are evaluated. This study uses these four parameters in tubes with different hole shapes. The highest force developed by the structure is known as the load-carrying capacity or LC. Considering the force-displacement curve, EA represents the energy the tube structure absorbs for a given displacement value. Therefore, EA can be explained as follows:

$$EA = \int_0^d F(y)\, dy \tag{1}$$

Where F(y) is the instantaneous load the tube structure carries, and d is the bending displacement. The specific energy absorption (SEA) is defined as the ratio of the energy absorbed by a structure to its mass, as presented in Eq. (2). In Eq. (2), m is the mass of the extrusion structure. This is a valid quantitative parameter, especially when comparing the performances of energy absorbers with different masses and geometries:

$$SEA = \frac{EA}{m} \tag{2}$$

4. Results and Discussions

Figure 5 compares the tubes' force (N) - displacement (mm) performances with different geometric hole shapes.

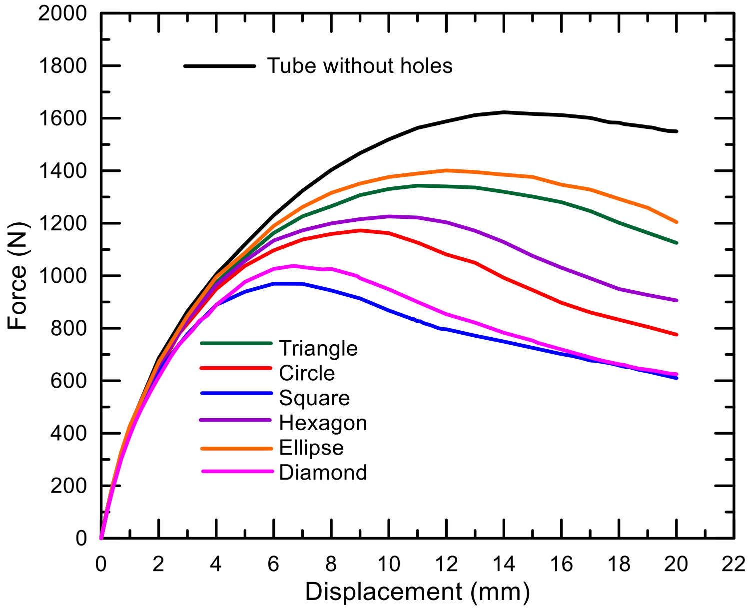

Figure 5. *Force-displacement curves of tubes with various hole shapes*

Figure 5 presents the load-displacement responses of aluminum tubes with and without perforations under bending conditions. The black curve represents the tube without holes, serving as a baseline for comparison. In contrast, the colored curves correspond to tubes with perforations of different geometrical shapes: triangle, circle, square, hexagon, horizontal ellipse, and diamond. As expected, the tube without holes exhibits the highest peak load, indicating superior structural integrity. This confirms that the introduction of perforations leads to a reduction in load-carrying capacity due to the localized stress concentrations and material removal. Among the perforated configurations, the tube with elliptical holes demonstrates the highest peak force, followed closely by the triangular hole configuration. These two geometries maintain a relatively high load-bearing capacity, suggesting a more favorable stress distribution around the perforations. The circular and hexagon configurations show intermediate performance. In contrast, the square and diamond hole configurations result in the most significant reduction in peak force, with the circular hole

configuration exhibiting the lowest load capacity. These shapes may cause more severe stress concentrations and material weakening under bending loads. Overall, the results indicate that the geometry of perforations plays a critical role in the structural response of tubes under bending. While perforations are often necessary for weight reduction or functional purposes, selecting an optimal hole shape, such as the horizontal ellipse or triangle, can mitigate strength degradation.
Simulation results obtained from finite element analyses are given in Table 2.

Table 2. *Simulation results obtained from finite element analyses ([a]Energy values are calculated up to 30 mm displacement)*

Specimen type	F_{max} (LC) (N)	Weight (g)	Specific load capacity (SLC) ($N.g^{-1}$)	Energy[a] (J) (EA)	Specific absorbed energy (SEA) ($J.g^{-1}$)
Tube without hole	1622	68.71	23,61	26.20	0,38
Triangle	1343	68.17	19,70	22.37	0,33
Square	970	67.44	14,38	15.18	0,23
Circle	1172	67.71	17,31	18.60	0,27
Ellipse	1401	68.23	20,53	23.32	0,34
Hexagon	1225	67.89	18,04	20.05	0,30
Diamond	1039	67.43	15.40	15.83	0.23

The tube without a hole exhibits the highest values for maximum load ($F_{\square ax}$) and absorbed energy (Energy). It also shows the highest specific metrics (SLC and SEA).
Among the specimens with holes, the ellipse generally performs the best in terms of both load capacity and energy absorption. The square has the lowest values in nearly every category, making it the weakest performer overall. The tube without a hole has the highest $F_{\square ax}$ (1622 N). The ellipse stands out among the shapes with holes (1401N), while the square has the lowest (970 N). SLC of the tube without a hole leads with 23.61 N/g, confirming its high strength-to-weight ratio. The ellipse follows at 20.53 N/g, and the triangles are close to each other in the mid-range. The square again is the lowest (14.38 N/g). The ellipse hole also absorbs the most energy (23.32 J). The triangle is next (22.37 J), with the square lowest (15.18 J). In terms of energy absorption per unit mass, the SEA of the ellipse still leads at 0.34 J/g. The Square and diamond remain the least efficient (0.23 J/g).
The von-Mises stress distribution of tubes with various hole shapes is shown in Figure 6. The tube (no hole) benefits from having no stress concentration zones, such as corners or openings, which helps distribute load evenly and enhances load capacity and energy absorption. Among the hollow shapes, the hexagon performs better than the shapes with fewer sides (Triangle, Square) or purely curved profiles (Circle, Ellipse), likely because of an effective stress distribution around its six edges and internal geometry. Shapes with sharp corners (Square, Triangle) typically introduce higher stress concentrations, explaining their lower load capacities and energy absorption values.

5. Conclusions

This paper presents a numerical investigation of the bending behavior of aluminum tubes with various hole shapes. The presence and shape of holes significantly affect the tube's structural strength. The best-performing perforated designs are those with elliptical and triangular holes, while square holes cause the most significant drop in load capacity. If maintaining strength while reducing weight is a priority, choosing the proper hole shape is crucial. Even though all specimens have very similar weights, their ability to carry the load and absorb energy varies significantly. If the aim is to maximize load carrying and energy absorption for a given weight, the ellipse perforated tube is the best choice among perforated tubes, followed by the triangular. The square is the least optimal choice here, showing the lowest load capacity and energy values.

Author Statements:

- **Ethical approval:** The conducted research is not related to either human or animal use.
- **Conflict of interest:** The authors declare that they have no known competing financial interests or personal relationships that could have appeared to influence the work reported in this paper

- **Acknowledgement:** The authors declare that they have nobody or no-company to acknowledge.

- **Author contributions:** The authors declare that they have equal right on this paper.

- **Funding information:** The authors declare that there is no funding to be acknowledged.

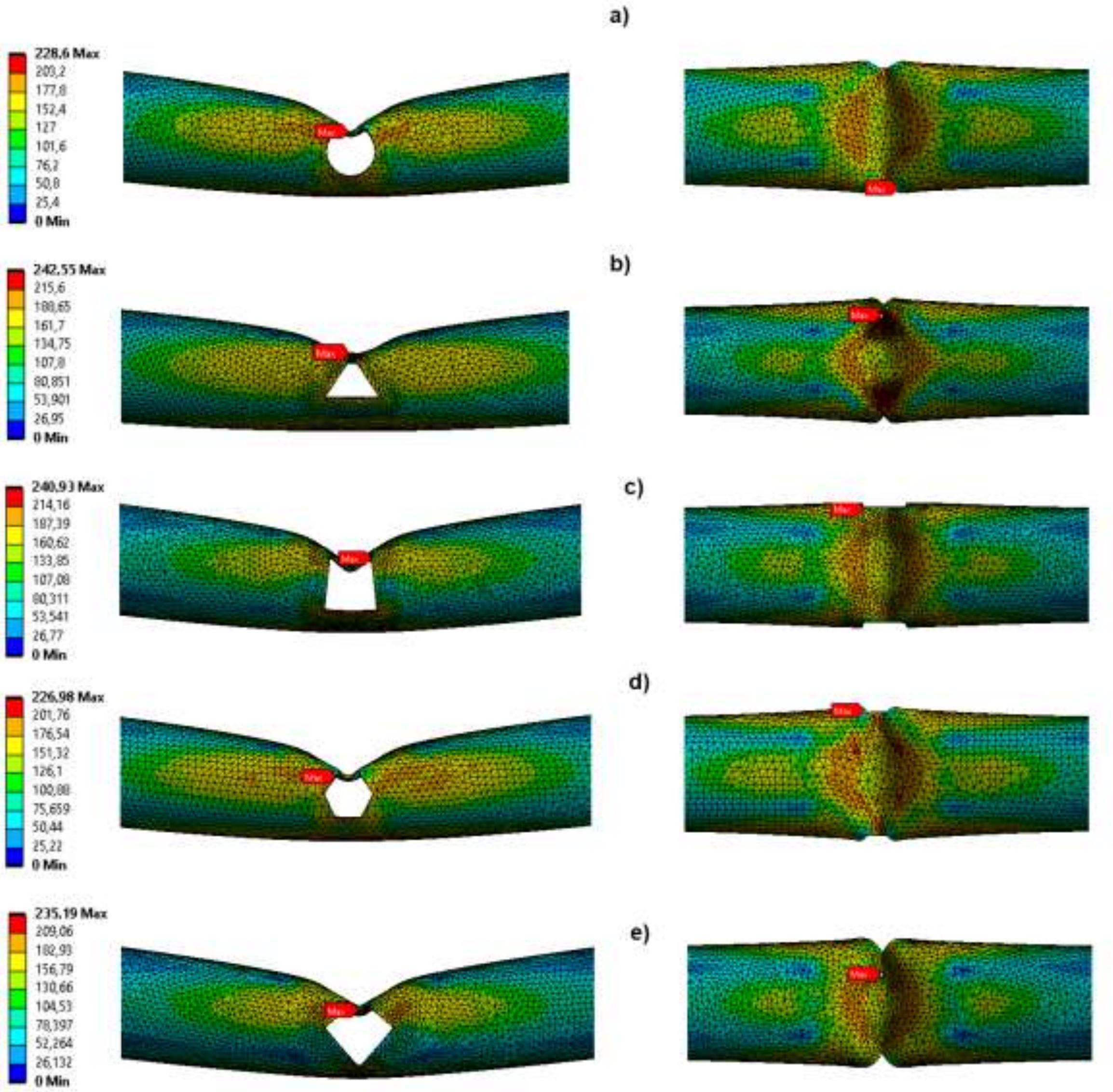

Figure 6. *Von-Mises stress distributions of the tube with various hole shapes, a) circle, b) triangle, c) square, d) hexagon, e) diamond*

- **Data availability statement:** The data that support the findings of this study are available on request from the corresponding author. The data are not publicly available due to privacy or ethical restrictions.

References

[1] Abramowicz, W., & Jones, N. (1986). Dynamic axial crushing of circular tubes. *International Journal of Impact Engineering*, 4(4), 243–270. https://doi.org/10.1016/0734-743X(86)90011-4

[2] Hanssen, A. G., Langseth, M., & Hopperstad, O. S. (2000). Static and dynamic crushing of circular aluminium extrusions with aluminium foam filler. *International Journal of Impact Engineering*, 24(5), 475–507. https://doi.org/10.1016/S0734-743X(99)00121-0

[3] Langseth, M., Hopperstad, O. S., & Hanssen, A. G. (1999). Crashworthiness of aluminium extrusions: Experiments and numerical analyses. *International Journal of Mechanical Sciences*, 41(3), 677–694. https://doi.org/10.1016/S0020-7403(98)00063-7

[4] Mamalis, A. G., Manolakos, D. E., Demosthenous, G. A., & Ioannidis, M. B. (1997). On the response of thin-walled square tubes to dynamic lateral loading. *International Journal of Mechanical Sciences*, 39(9), 989–1004. https://doi.org/10.1016/S0020-7403(96)00097-0

[5] Thornton, P. H., & Magee, C. L. (1993). Crash energy management in automotive structures. *International Journal of Impact Engineering*, 13(3), 227–239. https://doi.org/10.1016/0734-743X(93)90034-X

[6] Abramowicz, W. (2003). Thin-walled structures as impact energy absorbers. *Thin-Walled Structures*, 41(2–3), 91–107. https://doi.org/10.1016/S0263-8231(02)00081-0

[7] Chen, W., Lu, G., & Yu, T. X. (2009). Bending collapse of thin-walled square and rectangular aluminum alloy tubes. *Thin-Walled Structures*,

47(6–7), 739–749. https://doi.org/10.1016/j.tws.2008.12.014
[8] Yin, H. P., Fang, H., & Zhang, Y. Y. (2013). Numerical simulation of the bending behavior of aluminum alloy thin-walled square tubes. *Materials & Design*, 45, 454–462. https://doi.org/10.1016/j.matdes.2012.09.034
[9] Reyes, A., & Langseth, M. (2002). Crushing of circular aluminium tubes under axial loading. *International Journal of Mechanical Sciences*, 44(9), 1965–1984. https://doi.org/10.1016/S0020-7403(01)00157-7
[10] Kim, Y. J., Lee, S. H., & Wierzbicki, T. (2012). Crashworthiness of perforated circular tubes under axial compression. *Thin-Walled Structures*, 58, 61–73. https://doi.org/10.1016/j.tws.2012.04.008
[11] Hwang, Y. M., Su, H. C., & Chen, Y. M. (2014). Energy absorption characteristics of cylindrical tubes with various pre-folded patterns. *Materials & Design*, 57, 317–326. https://doi.org/10.1016/j.matdes.2013.12.059
[12] Attard, M. M., & Hunt, G. W. (2008). Experimental investigation of plastic buckling in aluminum tubes under bending. *Thin-Walled Structures*, 46(12), 1411–1419. https://doi.org/10.1016/j.tws.2008.03.009
[13] Singace, A. A., & El-Sobky, H. (1997). Behavior of axially crushed tubes with different modes of perforation. *Thin-Walled Structures*, 28(1), 79–90. https://doi.org/10.1016/S0263-8231(96)00029-7
[14] Ma, G. W., & Zhang, X. Y. (2003). Modeling of perforated plates under blast loading. *International Journal of Impact Engineering*, 28(4), 405–422. https://doi.org/10.1016/S0734-743X(02)00129-6
[15] Li, Z., Fang, J., & Yang, X. (2016). Crashworthiness of axially crushed aluminum alloy circular tubes with multiple holes. *Thin-Walled Structures*, 100, 155–166. https://doi.org/10.1016/j.tws.2016.01.007
[16] Alavi Nia, A., & Hoseini, S. M. (2011). Experimental and numerical investigation on the energy absorption characteristics of thin-walled tubes with different hole patterns. *Thin-Walled Structures*, 49(12), 1491–1500. https://doi.org/10.1016/j.tws.2011.08.008
[17] Kim, H. S., Kim, H. J., & Park, J. S. (2012). Numerical investigation of crashworthiness characteristics of thin-walled tubes with various holes. *Thin-Walled Structures*, 61, 17–29. https://doi.org/10.1016/j.tws.2012.06.005
[18] Hwang, Y. M., & Lin, Y. C. (2014). Performance of pre-folded energy-absorbing tubes under axial impact. *Materials & Design*, 54, 79–89. https://doi.org/10.1016/j.matdes.2013.08.057
[19] Ramu, I., & Senthil, R. (2017). Crushing behavior of aluminum tubes with holes under axial compression. *Materials Today: Proceedings*, 4(8), 8740–8746. https://doi.org/10.1016/j.matpr.2017.07.218
[20] Hou, S., Li, Q., Long, S., Yang, X., & Li, W. (2007). Crashworthiness design for foam-filled thin-wall structures. *Materials & Design*, 28(3), 1359–1362. https://doi.org/10.1016/j.matdes.2005.12.003
[21] Karagiozova, D., & Alves, M. (2004). Buckling of circular shells under dynamic axial compression. *International Journal of Solids and Structures*, 41(11–12), 3213–3234. https://doi.org/10.1016/j.ijsolstr.2004.01.001
[22] Tai, Y. S., Chu, T. C., & Huang, M. W. (2010). The crashworthiness performance of aluminum foam-filled tubes under oblique impact loading. *International Journal of Mechanical Sciences*, 52(11), 1474–1485. https://doi.org/10.1016/j.ijmecsci.2010.07.009
[23] Yang, S. S., Chen, J. H., & Pan, Y. (2015). Dynamic axial crushing behavior of foam-filled multi-cell thin-walled aluminum structures. *Composite Structures*, 133, 1–11. https://doi.org/10.1016/j.compstruct.2015.07.052
[24] Zarei, H. R., & Kröger, M. (2008). Multiobjective crashworthiness optimization of circular aluminum tubes. *International Journal of Mechanical Sciences*, 50(4), 903–913. https://doi.org/10.1016/j.ijmecsci.2007.09.008
[25] Li, Q., Yang, X., & Xu, Y. (2005). Energy absorption of structures and materials. *Applied Mechanics Reviews*, 58(6), 389–404. https://doi.org/10.1115/1.1992527
[26] Zarei, H. R., & Kröger, M. (2006). A numerical method for crashworthiness design of structures. *Thin-Walled Structures*, 44(9), 939–947. https://doi.org/10.1016/j.tws.2006.01.002
[27] Boria, S., Belingardi, G., & Koricho, E. G. (2016). Energy absorption capability of CFRP composite crash boxes with triggers. *Composite Structures*, 154, 318–330. https://doi.org/10.1016/j.compstruct.2016.07.049
[28] Fang, H., Zhang, Y., & Li, H. (2018). Numerical simulation of irregular-shaped holes on crashworthiness of square tubes. *International Journal of Mechanical Sciences*, 149, 109–123. https://doi.org/10.1016/j.ijmecsci.2018.10.017
[29] Zhao, B., & Elnashai, A. S. (2002). Seismic fragility assessment of RC structures in mid-America. *Mid-America Earthquake Center Report*.
[30] Kim, Y. J., & Wierzbicki, T. (2001). Crushing behavior of thin-walled hexagonal tubes. *International Journal of Mechanical Sciences*, 43(9), 2091–2116. https://doi.org/10.1016/S0020-7403(00)00123-5
[31] Russel, B. P., & McGregor, J. J. (2008). Experimental and numerical analysis of foam-filled metal tubes under bending loads. *International Journal of Impact Engineering*, 35(10), 998–1009. https://doi.org/10.1016/j.ijimpeng.2008.03.002
[32] Børvik, T., Langseth, M., Hopperstad, O. S., & Malo, K. A. (2001). Ballistic penetration of steel plates. *International Journal of Impact Engineering*, 27(1), 19–35. https://doi.org/10.1016/S0734-743X(01)00032-6
[33] Hamouda, A. M. S., & Hashmi, M. S. J. (1998). Testing and modeling of square thin-walled tubes subjected to axial loading. *Thin-Walled Structures*,

32(1–3), 1–28. https://doi.org/10.1016/S0263-8231(98)00022-6

[34] Lin, Y. C., Li, L., & Chen, M. S. (2010). Effects of strain rate on the compressive behavior of 5052-H38 aluminum alloy thin-walled tubes. *Materials Science and Engineering: A*, 527(3), 709–715. https://doi.org/10.1016/j.msea.2009.09.037

[35] Zhang, X., Wang, Z., & Wang, G. (2007). Numerical simulation of dynamic behavior of aluminum tubes under axial loading. *International Journal of Solids and Structures*, 44(15), 5029–5049. https://doi.org/10.1016/j.ijsolstr.2006.12.021

[36] Zhang, Y. X., & Yu, T. X. (2009). Progressive folding of square tubes under combined bending and axial loading. *Thin-Walled Structures*, 47(7), 784–791. https://doi.org/10.1016/j.tws.2008.11.004

[37] Kim, H. S., Youn, B. D., & Park, S. W. (2008). Collapse behavior of foam-filled square tubes with multiple cells. *International Journal of Mechanical Sciences*, 50(10–11), 1510–1519. https://doi.org/10.1016/j.ijmecsci.2008.07.009

[38] Belingardi, G., Cavatorta, M. P., & Koricho, E. G. (2011). Experimental investigation of CFRP composite crash boxes. *International Journal of Crashworthiness*, 16(4), 411–425. https://doi.org/10.1080/13588265.2011.591282

[39] Hanssen, A. G., Langseth, M., & Hopperstad, O. S. (2001). Static crushing of square aluminum extrusions with aluminum foam filler. *International Journal of Mechanical Sciences*, 43(1), 153–176. https://doi.org/10.1016/S0020-7403(99)00119-6